Surface Attachment of Horseradish Peroxidase to Nylon Modified by Plasma-Immersion Ion Implantation

Alexey Kondyurin,[1] Neil J. Nosworthy,[1] Marcela M. M. Bilek,[1] Robert Jones,[2] Paul J. Pigram[2]

[1]*Applied and Plasma Physics, School of Physics (A28), University of Sydney, Sydney, New South Wales 2006, Australia*
[2]*Centre for Materials and Surface Science and Department of Physics, La Trobe University, Melbourne 3086, Australia*

Received 27 August 2009; accepted 1 September 2010
DOI 10.1002/app.33355
Published online 10 January 2011 in Wiley Online Library (wileyonlinelibrary.com).

ABSTRACT: The surface of polyamide (nylon 6) was modified by plasma-immersion ion implantation (PIII) with nitrogen ions. Structural changes associated with carbonization, oxidation, and depolymerization were observed in the modified surface layer with Fourier transform infrared/attenuated total reflection (FTIR–ATR) spectroscopy, surface energy measurements, and X-ray photoelectron spectroscopy (XPS). The enzyme activity of surface-attached horseradish peroxidase was studied with a tetramethylbenzidine colorimetric activity assay. Compared to untreated controls, the PIII-treated surface showed a higher level of the attached protein with increased longevity of bioactivity. Detection of the immobilized protein layer was made difficult by the presence of amide groups in nylon. Here we demonstrate the potential of combining FTIR–ATR spectroscopy with XPS measurements for this purpose. © 2011 Wiley Periodicals, Inc. J Appl Polym Sci 120: 2891–2903, 2011

Key words: ESCA/XPS; FTIR; nylon; proteins; surfaces

INTRODUCTION

Nylon (polyamide), which was invented in 1928 by Wallace Carothers (DuPont), is a widely used engineering thermoplastic.[1–5] Nylon is created when a condensation reaction occurs between amino acids, dibasic acids, and diamines. The most popular kinds are nylon 6, nylon 6,6, and nylon 12. Nylon is characterized by strong hydrogen bonds between NH and C=O groups of polyamide macromolecule.[6] The dense packing of nylon macromolecules associated with hydrogen bonds leads to a high crystalline-fraction volume. The strong mechanical properties, high thermostability, high tribological stability, and high electrical isolation properties of nylon are exploited in machinery. Nylon is commonly used in the production of tire cords, rope, belts, filter cloths, sports equipment, and bristles. It is particularly useful when it is machined into bearings, gears, rollers, and thread guides. Thousands of custom nylon products can be found on the market.

One of the important application areas of nylon is medical devices. Nylon surgical sutures are well known and are used in surgery. Nylon surgical sutures are elastic, durable, mechanically stable *in vivo* for weeks, and nontoxic, do not cause inflammatory reactions, and are approved in a number of countries for application in medical implants.

The ability to strongly adsorb protein molecules onto the surface of a polymer implant and maintain a high degree of native bioactivity is believed to be important in achieving good biocompatibility. Unmodified polymer surfaces are usually not suitable for this kind of protein attachment, so the uppermost surface layer is typically modified by various chemical or physical methods. One method shown to be effective is ion-beam implantation and its variant, plasma-immersion ion implantation (PIII).

We have used PIII to improve protein attachment on ultrahigh-molecular-weight polyethylene (UHMWPE),[7] polytetrafluoroethylene,[8] and polystyrene.[9] The covalent bonding of a protein to the modified polymer surface has been observed with horseradish peroxidase (HRP), soybean peroxidase, and catalase. The bioactivity of the immobilized proteins is greatly increased longevity in comparison with the bioactivity on untreated controls. The preservation of catalytic activity indicates that the conformation of covalently attached proteins is better maintained on PIII-modified surfaces.

Ion-beam implantation and its variant PIII are based on collision and energy transfers from high-energy ions penetrating the polymer target. The depth of ion penetration depends on the kind of ion, its mass, and the density and atomic composition of the target. Usually, the energy of the ion is much higher than the energy required to break chemical

Correspondence to: A. Kondyurin (a.kondyurin@physics.usyd.edu.au).

Contract grant sponsor: Australian Research Council (for project costs and XPS instrumentation).

bonds in the polymer. Therefore, the penetrating ion breaks a number of bonds in macromolecules, sputters separate atoms and electrons from macromolecules, and excites the vibrational states of the macromolecules. A new chemical structure is then formed after displaced atoms and electrons come to rest and thermal energy has dissipated. A detailed overview of the relevant physical and chemical processes can be found elsewhere.[10–12]

Ion-beam implantation and PIII have been used for the modification of polyethylene,[13–21] polystyrene,[22–28] polytetrafluoroethylene,[29–34] poly(ethylene terephthalate),[35–38] poly(methyl methacrylate),[39–42] polyurethane,[43–47] and other polymers. Leading to increases in the hardness, electrical conductivity, and wettability, structural changes typical of ion-irradiated polymers, such as carbonization, depolymerization, and oxidation, have been observed.

In this study, we applied PIII modification to the polyamide nylon 6,6, a polymer routinely employed for medical applications. The structure and properties of nylon (or polyamide) have previously been investigated after ion-beam modification. Crosslinking and significant hardening have been reported.[48] Wettability and new chemical groups in the modified surface layer have been observed previously.[49] Chain scission was reported by Kumar et al.[50] Free radicals and high conductivity for ion-beam-implanted nylon were observed by Balasubramanian et al.[51] and Popok et al.[52] The carbonization and formation of π-electron clusters in nylon were observed after ion-beam implantation by Popok and coworkers.[53,54] Also, we reported carbonization, oxidation, and hardness improvements in a polyamide–polyether copolymer with PIII.[55]

After previous experience with protein attachment on other PIII-modified polymers,[7–9,12] which showed similar changes in their structure and properties, we expected an improvement in the protein attachment on ion-implanted nylon. Unfortunately, detection of the attached protein on nylon with Fourier transform infrared (FTIR) was difficult because of the similar chemical bonding in the protein backbone. This resulted in the same vibrational modes being present in the polyamide macromolecules and the protein molecules. We, therefore, report in this article the results of a different surface analytical strategy incorporating X-ray photoelectron spectroscopy (XPS), which resolved this issue and enabled us to demonstrate the improved protein binding properties arising from the PIII modification.

EXPERIMENTAL

Polyamide nylon 6,6 film (medical application grade) was purchased from McMaster-Carr (Chicago, IL, United States). Nylon strips (20 mm × 50 mm × 1 mm) were washed with ethanol and dried for several days before use. HRP (product code P6782) was purchased from Sigma–Aldrich (Castle Hill, NSW, Australia).

PIII was conducted in inductively coupled radio-frequency (13.56 MHz) plasma in nitrogen gas (99.99%). The base pressure in the plasma vessel was 10^{-4} Pa. The nitrogen flow rate was regulated in the range of 80–120 sccm to achieve a constant pressure of 4.4×10^{-2} Pa during implantation. The radio-frequency plasma power was 100 W, and the reverse power was 12 W when they were matched. The plasma density during treatment was continuously monitored with a Langmuir probe with a radio-frequency block (Hiden Analytical, Ltd., Warrington, UK). The acceleration of ions from the plasma was achieved by the application of high-voltage (20-kV) bias pulses of 20-μs duration to the sample holder at a frequency of 50 Hz. The plasma treatment system was designed and constructed in house, and a PI^3 high-voltage power supply was purchased from the Australian Nuclear Science and Technology Organisation (Sydney, NSW, Australia). A schematic diagram and a photograph of the PIII system used are shown elsewhere.[12]

The samples were mounted onto a stainless steel holder with a stainless steel mesh electrically connected to the holder, which was placed 45 mm in front of the sample surface. The samples were treated for durations of 20–800 s, which corresponded to implantation ion fluences of $0.5–20 \times 10^{15}$ ions/cm^2. The ion fluence was calculated from the number of high-voltage pulses multiplied by the fluence corresponding to one pulse. The fluence of one high-voltage pulse was determined by a comparison of ultraviolet transmission spectra of polyethylene films implanted under the conditions used here and spectra of samples implanted with known ion fluences in previous PIII and ion-beam treatment experiments.[12]

The wettability of the nylon samples was measured with the sessile drop method with a Kruss DS10 contact-angle instrument (KRUSS GmbH, Hamburg, Germany). Deionized water and diiodomethane were the test fluids. The surface energy and its components (polar and dispersive parts) were calculated with the Owens–Wendt–Rabel–Kaelble, Fowkes, and Wu methods. Wettability measurements were undertaken 60 min after the PIII treatment of nylon, which comprised 30 min in the vacuum chamber with a residual pressure of 10^{-3} Pa and 30 min in air.

After the PIII treatment, the nylon samples were stored for 30 days in air-filled, closed containers at room temperature (stabilized at 23°C). After 30 days, the nylon samples were incubated overnight in an HRP solution (50 μg/mL in a 10 m*M* sodium

phosphate buffer, pH 7) at 23°C. The incubation time was selected according to experience from previous experiments with UHMWPE and polystyrene, which showed that the protein absorption saturated after approximately 1 h.[56] Overnight incubation was convenient and ensured that saturation had been reached. After incubation, nylon samples were washed six times (20 min for each wash) in a buffer solution (10 m*M* sodium phosphate buffer, pH 7). Samples for FTIR spectroscopy analysis were washed in deionized water for 10 s for the removal of buffer salts from the nylon surface.

The HRP activity was measured via the clamping of the nylon samples (13 mm × 15 mm) between two stainless steel plates separated by an O-ring (inner diameter = 8 mm, outer diameter = 11 mm), which was sealed to the plasma-treated surface. The top plate contained a 5-mm-diameter hole. 3,3,5,5′-Tetramethylbenzidine (TMB; T0440, Sigma, Castle Hill, NSW, Australia) was added to the polymer surface. After 30 s, 25 μL was removed and added to 50 μL of 2*M* HCl; this was followed by 25 μL of unreacted TMB to bring the volume to 100 μL. The optical density was then measured at a wavelength of 450 nm with a Beckman DU 530 spectrophotometer (Beckman, Gladesville, NSW, Australia).

Fourier transform infrared/attenuated total reflection (FTIR–ATR) spectra of the nylon samples were recorded with a Digilab FTS7000 FTIR spectrometer (Holliston, MA, USA) fitted with an attenuated total reflection accessory (Harrick, Pleasantville, NY, USA) and a trapezium germanium crystal with an incidence angle of 45°. The generation of spectra with a sufficiently high spectral band resolution and signal-to-noise ratio required 500 scans at a resolution of 1 cm^{-1}. The surface of the nylon was dried with a dry air flow before data collection. Differences (obtained by subtraction) between the spectra of samples taken before and after the PIII treatment were used to characterize the effects of surface treatments. All spectral analyses were undertaken with GRAMS software (ThermoFisher, Waltham, MA, USA).

Micro-Raman spectra were recorded in a backscattering mode excited by Nd:YAG laser irradiation (2 ω, wavelength = 532.14 nm) on a diffraction double-monochromator spectrometer (HR800, Jobin Yvon) with the LabRam 010 system (Lastek, Adelaide, SA, Australia). An optical microscope was used for focusing the exciting laser beam and for collecting the Raman scattered light. An objective of 100 units was used. The sample surface position alignment during the Raman signal acquisition was adjusted according to an image projected onto a screen from a microscope-mounted charged coupling device camera. The intensity of the laser beam was adjusted to avoid overheating of the samples. A spectral resolution of 4 cm^{-1} was used. The number of scans was selected from the range of 100–4000 to provide a sufficient signal/noise ratio for the spectra. LabRam software was used for spectral analysis.

XPS measurements were performed with an Axis Ultra DLD spectrometer (Kratos Analytical, Manchester, UK) equipped with a monochromatized X-ray source (Al Kα, $h\nu$ = 1486.6 eV) operated at 150 W, a hemispherical analyzer, and a delay line detector. The spectrometer energy scale was calibrated with the $Au_{4f7/2}$ photoelectron peak at the binding energy of 83.98 eV. One-scan survey spectra were acquired for binding energies in the range of 0–1400 eV at a pass energy of 160 eV with a dwelling time of 0.25 s. C_{1s}, O_{1s}, and N_{1s} region spectra were acquired at a pass energy of 20 eV for higher spectral resolution. Peaks were fitted with synthetic Gaussian (70%)–Lorentzian (30%) components with the Marquardt–Levenberg fitting procedure of the Kratos Analytical and CasaXPS data processing packages. Peaks were quantified with relative sensitivity factors supplied by the spectrometer manufacturer. Linear background subtraction was used, and the spectra were charge-corrected with the C_{1s} C—C/H component set to 285.0 eV. The analysis area was 700 μm × 300 μm. Surface etching of selected samples was achieved with 5-keV Ar^+ ions raster-scanned over an area of 2.5 mm × 2.5 mm.

Some XPS measurements were repeated with a spectrometer (Specs, Berlin, Germany) equipped with an Al X-ray source with a monochromator operated at 200 W, a hemispherical analyzer, and a line delay detector with nine channels. Survey spectra were acquired for binding energies in the range of 0–1200 eV at a pass energy of 30 eV. C_{1s}, O_{1s}, and N_{1s} region spectra were acquired at a pass energy of 23 eV with 10 scans to obtain a higher spectral resolution and to lower the noise level. S_{2p} region spectra were acquired at a pass energy of 30 eV with 50 scans and a 0.5-s dwelling time to obtain even lower noise levels.

RESULTS AND DISCUSSION

Structural transformation due to the PIII treatment

Figure 1 shows micro-Raman spectra of untreated and PIII-treated nylon. The spectrum for untreated nylon has narrow lines attributed to the vibrational modes of the polymer macromolecules at 1639, 1443, 1300, 1236, 1132, 1064, and 954 cm^{-1}. With the PIII treatment, the Raman spectrum changes dramatically. The line intensity is lower, and a broad background between 1200 and 1600 cm^{-1} appears. The background is formed by two wide bands (the G-peak and the D-peak) attributed to vibrations in graphitic structures. Such background features are

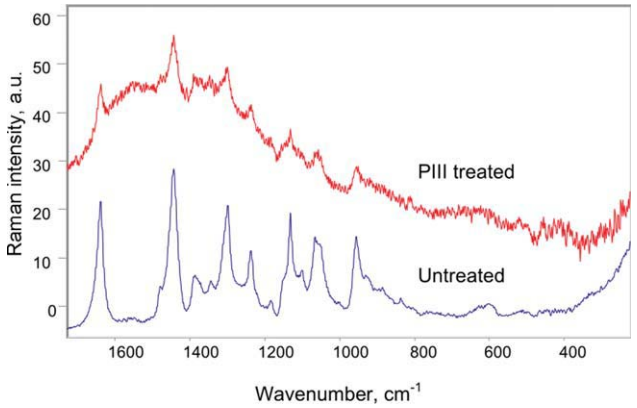

Figure 1 Micro-Raman spectra of untreated nylon and nylon after the PIII treatment. [Color figure can be viewed in the online issue, which is available at wileyonlinelibrary.com.]

observed in the spectra of most other polymers after ion-beam implantation.[12] Visually, the nylon surface becomes darkened after the PIII treatment with high ion fluence (10^{15}–10^{16} ions/cm^2). At lower ion fluences (<10^{15} ions/cm^2), no effect is visible. The darkening of the surface layer is caused by carbonization and is consistent with the formation of the graphitic structures observed in the corresponding micro-Raman spectrum (Fig. 1). Carbonization of the surface layer is the reason for the appearance of cracks on the surface, as discussed in our previous study.[55] The density of the cracks is low and does not significantly increase the effective surface area of the nylon.

FTIR–ATR spectra of untreated nylon show a series of characteristic and well-known bands corresponding to vibrations of amide groups. These include the amide A line (3302 cm^{-1}), the amide B Fermi resonance line (overtone of N—H bending; 3080 cm^{-1}), the amide I line (1634 cm^{-1}), the amide II line (1540 cm^{-1}), the amide III line (1276 cm^{-1}), and the amide IV line (936 cm^{-1}; Fig. 2). These lines are attributable to amide groups with strong hydrogen bonds. The presence of hydrocarbon chains is indicated by lines corresponding to C—H stretching vibrations at 2935 and 2860 cm^{-1} and to bending vibrations in —CH_2— groups at 1474, 1466, and 1418 cm^{-1}.

As for the micro-Raman spectra, the FTIR–ATR spectra change dramatically after the PIII modification of nylon. The broad background band in the 1500–1000-cm^{-1} region, with a maximum at 1250 cm^{-1}, grows with ion fluence. This band is attributable to vibrations in highly carbonized structures, which appear in the surface layer after ion-beam implantation. This is consistent with the observations of the micro-Raman study and previous studies.[12] This band is broad and unstructured because of the irregular character of the carbon bonds forming as a result of the PIII treatment.

The intensity of the amide A, B, I, and II lines decreases with the ion-beam fluence. Additional absorbance lines appear in the high-frequency region (3600–3000 cm^{-1}) and in the middle-frequency region (1800–1500 cm^{-1}). Spectral changes associated with PIII treatment are highlighted by the subtraction of the equivalent untreated nylon spectrum (inset in Fig. 2). Complete subtraction of all nylon peaks is impossible because of peaking shifting. Additional lines at 3629, 3378, 3164, and 3031 cm^{-1} appear and increase with the ion fluence. According to the accepted interpretation of polyamide spectra, these lines may be attributed to hydroxyl group vibrations (3629 cm^{-1}), amide and amine group vibrations (3378 and 3164 cm^{-1}), and C—H stretching vibrations in unsaturated carbon structures (3031 cm^{-1}). These spectral changes indicate that the PIII treatment breaks bonds associated with amide groups and results in the formation of amine, hydroxyl, and unsaturated C=C groups in the nylon surface layer.

A line at 2215 cm^{-1} that is attributed to stretching vibrations of newly formed C≡N groups appears with the PIII treatment. In the region of 1715 cm^{-1}, which is characterized by a strong line arising from carbonyl group vibrations, the absorbance increases with the ion fluence. Such groups exist in untreated nylon, and the carbonyl group line (amide I) of nylon can be observed in the spectra of unmodified samples. In the spectra obtained from PIII-modified samples, the high-frequency shoulder of the amide I line becomes stronger, and this is indicative of the generation of new carbonyl groups not associated with those found in untreated nylon. In addition to the appearance of new chemical functional groups, there is a significant decrease in the intensity of the 1474- and 1418-cm^{-1} lines with the ion fluence. These lines are attributable to C—H bending

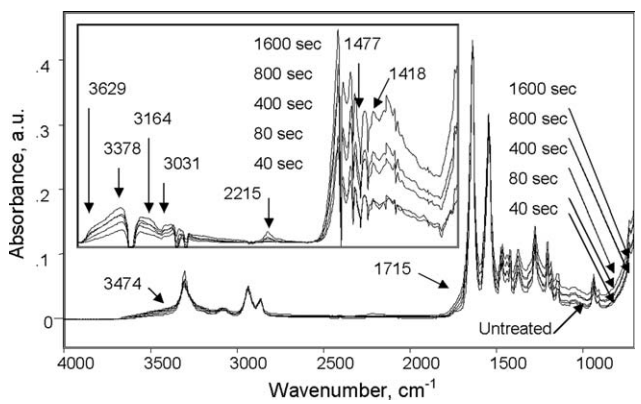

Figure 2 FTIR–ATR spectra of nylon after the PIII treatment. The PIII treatment times are noted from bottom to top (untreated and 40, 80, 400, 800, and 1600 s). The inset shows difference spectra from untreated and treated samples with PIII treatment times of 40, 80, 400, 800, and 1600 s.

vibrations in the aliphatic part of the nylon macromolecule near the amide group.

The spectra show that the structure of the nylon polymer is significantly transformed by chemical reactions resulting from the PIII modification. A penetrating ion with high energy undergoes a number of collisions with nylon macromolecules and results in the ejection of molecular fragments and ions containing carbon, oxygen, nitrogen, and hydrogen atoms in addition to the emission of secondary electrons. As a result, highly reactive free radicals are formed in the polymer surface layer. These trigger a number of chemical reactions that give rise to new structures in a process often called ion-beam damage. According to reactions known to occur in photo- and radiation-damaged nylon,[57,58] we propose analogous reactions as first approximations of the chemical changes occurring in PIII-modified nylon.

The radicals generated in the aliphatic part of the nylon macromolecules react in the same way as those in saturated hydrocarbons. Such radicals can move along the macromolecule chain and cause structural transformations in layers deeper than the ion-penetration depth. After the removal of treated nylon samples from the vacuum chamber into air, these radicals react with atmospheric oxygen and water and result in the formation of hydroxyl, carboxyl, carbonyl, and aldehyde groups. This gives rise to the appearance of lines at 3629, 3031, and 1715 cm^{-1} in the spectra of modified nylon. A detailed analysis of these reactions can be found elsewhere.[12]

The presence of the nylon amide group provides more potential for chemical transformations than the saturated hydrocarbon group. A loss of hydrogen from the methylene group joined to the amide group can be observed, and this results in a significant decrease in the number of such methylene groups and an accompanying decrease in the intensity of the 1477- and 1418-cm^{-1} spectral lines:

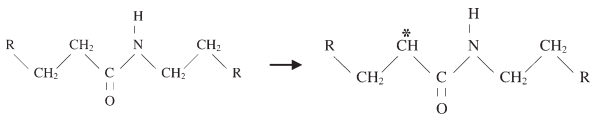

(1)

or

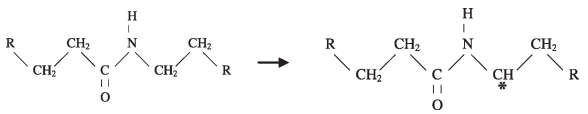

(2)

The appearance of a free radical at the carbonyl group usually causes a dissociation of this group from the macromolecule and the release of CO (in the gas phase):

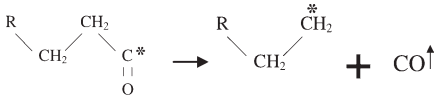

(3)

The carbonyl radical may be transformed into aldehyde, carboxyl, or hydroxyl groups when a proton donor radical is close enough to be involved in the reaction. An aminyl radical can react with another free radical to form a secondary amine group or be transferred to a primary amine group:

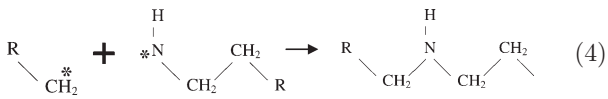

(4)

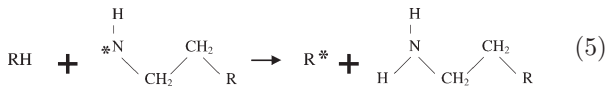

(5)

The appearance of amino acid groups may occur in the following way:

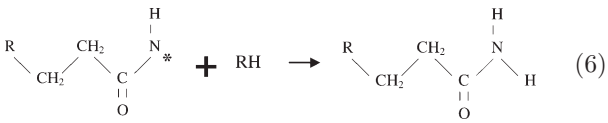

(6)

The occurrence and progress of these reactions may be followed with the 3629-, 3378-, and 3164-cm^{-1} spectral lines. Dehydration of the amide group yields a nitrile group, which is indicated by the appearance of the 2215-cm^{-1} spectral line:

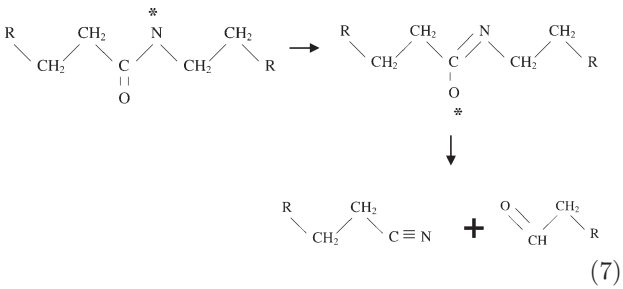

(7)

The appearance of nitrile groups may also be caused by the reaction of sputtered nitrogen and carbon atoms:

(8)

The intensity of the observed vibrational lines was analyzed as a function of the ion-beam fluence (Fig. 3). The intensity of the 2933-cm^{-1} line, which corresponds to $-CH_2-$ group stretching vibrations in the nylon macromolecules, was used as an internal standard. The number of new carbonyl groups

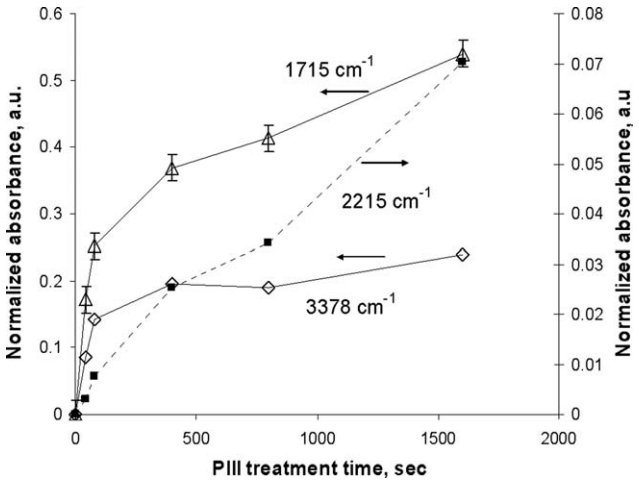

Figure 3 Absorbance of lines in the FTIR–ATR spectra of nylon after the PIII treatment: 3378 (amide and amine groups), 2215 (nitrile group), and 1715 cm^{-1} (carbonyl group). The absorbance of these lines was normalized to the absorbance of the 2933-cm^{-1} line corresponding to the —CH_2— group stretching vibration in the nylon macromolecule.

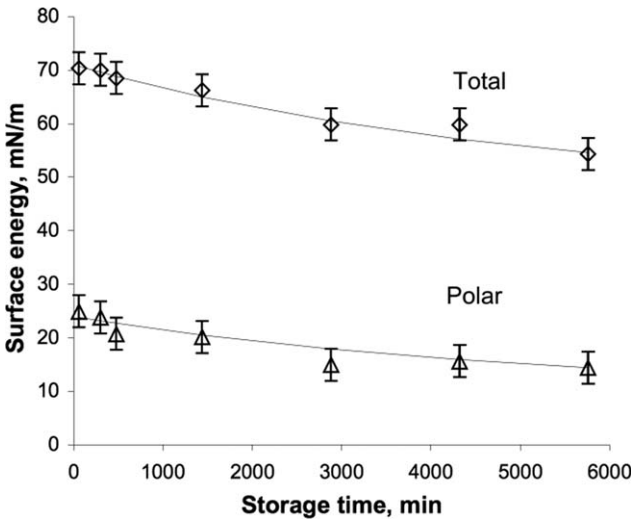

Figure 5 Total and polar surface energies of nylon after the PIII treatment as functions of the storage time in air. The data points show the experimentally measured values, whereas the curves show the best fits obtained through the fitting of an exponential function.

increases with the ion-beam fluence, as observed from changes in the 1715-cm^{-1} line intensity. At low fluence, the number of carbonyl groups increases sharply. However, at high ion fluence, the rate of the increase in carbonyl groups is slowed. The number of new amide and amine groups increases at low fluence and remains constant at high fluence. The number of nitrile groups grows continuously with increasing ion-beam fluence. The number of neighboring methylene groups decreases significantly at low fluence and remains constant at high fluence (Fig. 4).

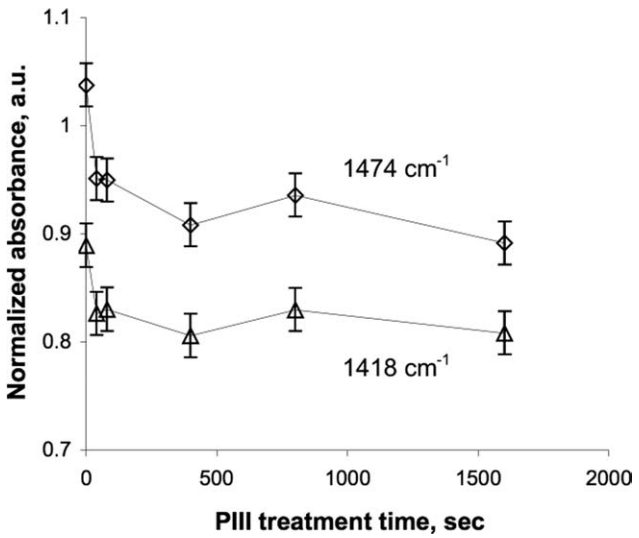

Figure 4 Absorbance of the 1474- and 1418-cm^{-1} methylene group lines in the FTIR–ATR spectra of nylon after the PIII treatment. The absorbance of these lines was normalized to the absorbance of the 1466-cm^{-1} line.

Such kinetics shows that the structural transformations in nylon caused by PIII treatment have a complex character with at least two different stages apparently depending on the ion fluence. During the first stage (fluence $\leq 10^{15}$ ions/cm^2), new groups appear, and some native groups disappear. This stage is characterized by substantial structural transformations, which involve amide, amine, hydroxyl, and carboxyl groups. During the second stage (fluence $>10^{15}$ ions/cm^2), smaller structural transformations occur with ion-beam fluence, and these transformations do not depend strongly on the fluence.

These two stages are consistent with structural transformations observed in other polymer systems exposed to PIII treatment. For example, polystyrene films are strongly oxidized and etched at low ion fluence. At high fluence, the surface layer becomes carbonized, and structural transformations can occur only in the deeper layers. Similarly, the PIII modification of nylon causes structural transformations of nylon macromolecules at low fluence, whereas at high fluence, the surface layer becomes carbonized, and further structural transformations observed in the spectra occur in deep layers: they are driven not by high-energy primary ions but rather by free radicals moving into the material from the disrupted surface layer.

Structural transformations in the surface layer change the surface energy of nylon. The wettability changes significantly after PIII modification. The water contact angle decreases from 76.2° for the untreated material to 35.3° after the PIII treatment, and the surface energy and its polar and dispersive

TABLE I
Parameters of the Fitted Total and Polar Surface Energies of PIII-Treated Nylon as Functions of the Storage Time

Parameter	Total	Polar
σ_1 (mN/m)	24	14
t_0 (1/min)	5000	5000
σ_∞ (mN/m)	47	10

$$\sigma = \sigma_1 \cdot \exp\left(-\frac{t}{t_0}\right) + \sigma_\infty$$

components change. The surface energy of untreated nylon has been calculated to be 44.2 mN/m. After the PIII treatment, the surface energy (calculated by the Owens–Wendt–Rabel–Kaelble method) increases to 70 mN/m (Fig. 5). Most of the change occurs in the polar component and is driven by new polar groups appearing in the surface layer after the PIII treatment. The polar component of the surface energy (calculated with the Owens–Wendt–Rabel–Kaelble method) increases from 2.7 mN/m for untreated nylon to 24 mN/m for PIII-treated nylon. Similar results can be observed with the Fowkes and Wu methods for surface energy calculations: the total energy for PIII-treated nylon is 70.3 and 76.4 mN/m, respectively, and the polar part is 24.9 and 30.8 mN/m, respectively.

Hydrophobic recovery

The wettability and surface energy are not stable with time after the PIII treatment. The water contact angle increases with the storage time in air. After 1 week, the wettability stabilizes and is characterized by a water contact angle of 58.4°.

The increase in the surface energy after PIII is caused by chemical transformations at the modified nylon surface and, in particular, the appearance of high-energy polar groups. The decrease in the surface energy observed after storage of the modified material may have the same origin as similar surface energy decreases observed after plasma polymerization or plasma treatment of polymer surfaces[59–61] (including plasma-treated nylon surfaces).[62] Accepted models for surface energy decreases and hydrophobicity recovery with time in these plasma-treated polymers discuss the reptation or diffusion of the surface polymer chains and the rotation of high-energy surface functional groups back into the polymer bulk.[63] First, variation of the wettability with time, depending on the environment, has been observed for copolymers and gel-like polymers; the mobility of macromolecules is high, and phase separation plays a significant role in surface-layer formation.[64,65] Moreover, the same model of surface-layer mobility has been used for the explanation of wetting recovery in plasma-treated polymers.[66] The surface energy of plasma-treated polymers is thereby reduced, and the hydrophobicity is increased. However, in the case of PIII treatment, the diffusion of polymer chains, as in the reptation picture, would be hindered by the dense crosslinking associated with highly carbonized structures appearing after high fluence modification.

Another possible pathway may be the adsorption of adventitious carbon and hydrocarbons on the activated surface with atmospheric exposure.[67] The changes in wettability in this study were repeatable despite the variable nature of the uncontrolled laboratory atmosphere, and the FTIR–ATR spectra did not show any significant growth in lines attributed to adsorbed hydrocarbons on the surface.

The most realistic explanation is that the changes in the surface energy observed with the storage time after modification are associated with chemical changes and/or structural relaxation at the surface of the modified nylon. The character and kinetics of these transformations are complex and depend on a number of reactions characterized by different rates of reaction.

The principle of macrokinetics may be applied to simulate these transformations. These relaxation processes may be fitted with exponential functions that correspond to first-order reactions. An exponential function was fitted to the polar component of the surface energy (σ), and agreement between the experimental data and the theoretical curve was found (Fig. 5). The fitted curve was determined as follows:

$$\sigma = \sigma_1 \cdot \exp\left(-\frac{t}{t_0}\right) + \sigma_\infty$$

where t is the time after PIII treatment, σ_1 is the constant, t_0 is the characteristic time of the surface energy decay and σ_∞ is the surface energy of the modified nylon after an infinite storage time. The value of $\sigma_1 + \sigma_\infty$ is the surface energy of modified nylon immediately after the PIII treatment (Table I).

The characteristic time shows that the wettability of the modified nylon is stabilized 3.5 days after the PIII treatment. The surface energy after an infinite storage time (47 mN/m with a 10 mN/m polar component) does not return to the value for the untreated nylon surface (44.2 mN/m with a 2.7 mN/m polar component). The change in the surface energy is determined mostly by the polar component. The dispersive component of the surface energy remains in the range of 40–47 mN/m for untreated and modified nylon surfaces.

The total surface energy immediately after the PIII treatment (71 mN/m) is high for polymers and organic substances. Usually, the total surface energy

TABLE II
Binding Energy (E_b) Values and Atomic Fractions Measured from Survey Spectra of the Samples

Sample	Atomic fraction (%)							
	Na_{1s} (1071 eV)	$Fe_{2p3/2}$ (712 eV)	O_{1s} (531 eV)	N_{1s} (400 eV)	$Ca_{2p3/2}$ (347 eV)	C_{1s} (285 eV)	S_{2p} (165 eV)	P_{2p} (133 eV)
Untreated	0.04	<0.01	11.3	11.0	<0.01	77.1	0.03	0.03
PIII-treated	0.03	1.03	12.0	14.0	0.12	72.4	0.04	0.01
Untreated and soaked in the buffer	<0.01	<0.01	11.5	10.6	<0.01	77.9	<0.01	<0.01
PIII-treated and soaked in the buffer	0.87	0.12	14.8	9.8	0.2	74.4	0.01	0.10
Untreated and soaked in the HRP solution	0.11	<0.01	13.4	11.6	<0.01	74.9	0.06	0.04
PIII-treated and soaked in the HRP solution	0.69	0.23	15.6	12.1	0.2	71.2	0.10	0.15

The noise level was approximately 0.01%. The E_b values are shown in parentheses ($\Delta E_b = \pm 1$ eV).

for high-energy organic surfaces does not exceed 45–50 mN/m. There are two possible sources for the high surface energy: newly introduced polar groups and free radicals. An examination of the literature shows that surface energies as high as 71 mN/m cannot be explained by the coverage of new polar groups that we have observed. The reported surface energies are considerably lower for polar polymers such as poly(methyl methacrylate) with a high concentration of C=O groups in the backbone (49 mN/m), polycarbonate with aromatic rings and carbonyl groups in the backbone (46.7 mN/m), and poly(ether ester ketone) with ether, ester, and aromatic ring groups in the backbone (46 mN/m). In all of these cases, the surface energy does not exceed 50 mN/m.[68]

The value that we have measured (71 mN/m) is close to that for inorganic substances such as ceramics and metals. The surface energy of carbon structures such as graphite and diamond depends on the presence of dangling bonds at the surfaces. In the case of hydrogenated and oxidized surfaces of diamond and graphite, surface energies of 47 and 65.8 mN/m, respectively, have been reported.[69] A low surface energy has been observed for fullerenes, which do not have unbonded electrons at the surface (48.1 mN/m),[70] and carbon nitrides (51.9–41.9).[71] However, the surface energy of carbon structures terminated with unbonded electrons has been reported to be in the range of 4000–1000 mN/m.[72,73] This high surface energy arises from the presence of free radicals in the surface layer. Free, uncoupled electrons create strong intermolecular interactions, as observed for metal surfaces, which have surface energies in the range of 100–1000 mN/m;[74] these correspond to complete coverage of the metal surface by the free electron cloud. The same high-density free electron gas is responsible for the high surface energy of intrinsic graphite, which has been reported to be 1750 (experimental measurement)[75] and 3338 mN/m (calculation).[76] We do not expect such high coverage of the surface of our modified nylon by free electrons associated with free-radical groups; however, the high surface energy does indicate that the PIII treatment results in the generation of a significant number of free radicals at the freshly treated polymer surface. The presence and disappearance of free radicals on the modified nylon surfaces change the polar component of the surface energy and not the dispersive component as expected of the strong polar electrostatic interactions of free, uncoupled electrons.

Therefore, we propose that most of the changes in the wettability and surface energy of PIII-modified nylon are produced by free radicals in the top layer, which is in contact with the wetting liquid. Residual differences in the surface energy for untreated and PIII-modified nylon after long storage times are connected to stable groups that appear after the completion of the free-radical reactions. The same effect of surface energy changes in polyethylene after the PIII treatment was observed and discussed previously.[21]

XPS analysis

Changes in the composition and chemical state at the surface may be revealed by XPS. XPS is complementary to FTIR–ATR because it is sensitive to shallow depths of approximately 10 nm, whereas FTIR–ATR samples regions up to a few micrometers. In the case of nylon, we cannot rely on FTIR–ATR to detect a surface-attached protein monolayer because of the presence of amide peaks in the polymer. We examined two strategies. With the first method, we performed high-resolution elemental scans of the C_{1s}, O_{1s}, and N_{1s} peaks and detected the differences in the bonding state of the ion-modified nylon and the protein layer on top. Such an analysis is not possible with FTIR–ATR because of the contribution of the unmodified bulk regions of the nylon to the signal. With the second strategy, we explored the use of the sulfur peak to detect the protein layer.

Table II shows the relative atomic concentrations at the surface derived from XPS survey spectra (not shown) for a sequence of six sample types: untreated

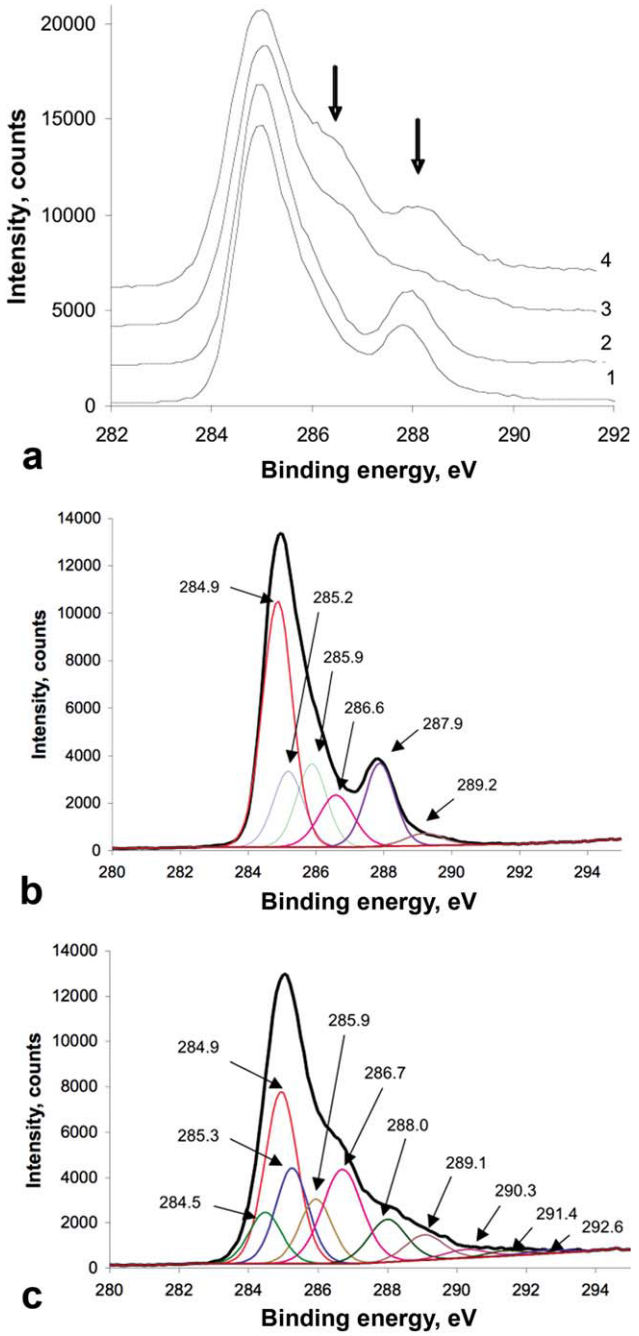

Figure 6 (a) XPS C_{1s} lines of untreated nylon incubated in (1) the buffer or (2) the HRP-containing buffer and PIII-treated nylon incubated in (3) the buffer or (4) the HRP-containing buffer, (b) XPS C_{1s} lines of untreated nylon fitted by individual lines, and (c) XPS C_{1s} lines of PIII-treated nylon fitted by individual lines. [Color figure can be viewed in the online issue, which is available at wileyonlinelibrary.com.]

and PIII-treated nylon samples; untreated and PIII-treated nylon samples immersed in a buffer and rinsed in water; and untreated and PIII-treated nylon samples immersed in an HRP solution, washed in a buffer, and rinsed in water. As expected, the principal constituents are carbon, nitrogen, and oxygen. The fact that changes to the spectra are not affected by rinsing indicates that the modified layer is a crosslinked, bonded network rather than free molecular fragments.

The spectrum of untreated nylon, in agreement with the reference data,[69] contains C_{1s}, O_{1s}, and N_{1s} lines. The lines are multiplets corresponding to the nylon macromolecule structure. Figures 6–8 show that significant changes in the C_{1s}, O_{1s}, and N_{1s} lines can be observed after the PIII treatment.

The C_{1s} shoulder near 288 eV in the spectrum of untreated nylon, attributed to carbon in the amide group of the nylon macromolecule, is diminished by the PIII treatment, and a new shoulder at 286 eV appears. The main peak at 284.9 eV broadens on the low binding energy side (284.5 eV) and corresponds to graphitization and carbonization of the nylon. Graphitization is further supported by the appearance of a shake-up satellite intensity around 292 eV, which is associated with the formation of aromatic structures. The amide component (binding energy = 288 eV) is significantly reduced with the PIII treatment. A similarly significant increase in the C—O/C≡N component occurs, and this is consistent with the PIII transformation of amide groups into nitrile groups and carbonyl species. Component peaks are enhanced with the PIII treatment at binding energies of 289 and 290 eV, which correspond to carboxyl and carbonate-like groups.

The untreated nylon sample exhibits intense, narrow O_{1s} and N_{1s} component peaks corresponding to the amide linkages (O=C—NH—). The O_{1s} envelope broadens after PIII modification toward the high-energy region and shows several additional component peaks with higher energy. This behavior is consistent with the formation of new oxygen-containing species, as observed in the C_{1s} spectra. The

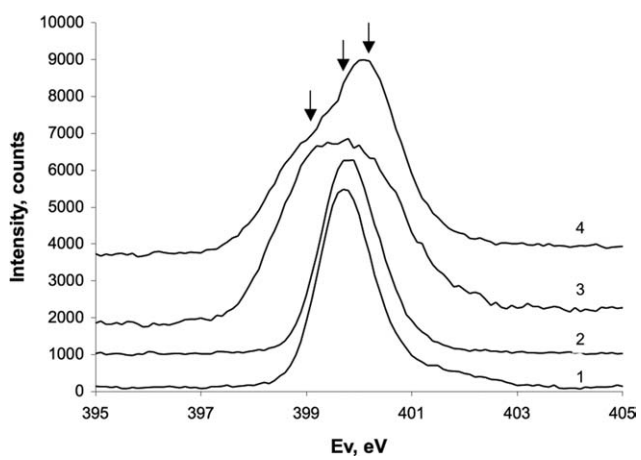

Figure 7 XPS N_{1s} lines of untreated nylon incubated in (1) the buffer or (2) the HRP-containing buffer and PIII-treated nylon incubated in (3) the buffer or (4) the HRP-containing buffer.

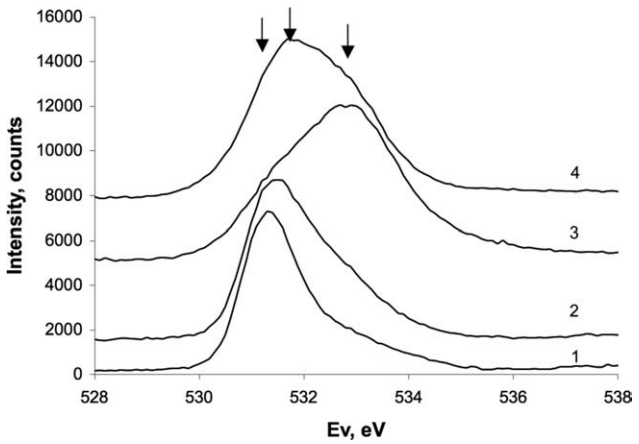

Figure 8 XPS O_{1s} lines of untreated nylon incubated in (1) the buffer or (2) the HRP-containing buffer and PIII-treated nylon incubated in (3) the buffer or (4) the HRP-containing buffer.

N_{1s} line broadens (Fig. 7) because of the appearance of nitrogen atoms associated with carbonyl or carboxyl groups and possibly charged nitrogen species. After the PIII treatment, contributions corresponding to amine and C≡N groups can be observed, and these are consistent with the evolution of similar bonds observed by FTIR. NO and NO_2 components could also contribute to the observed broadening of N_{1s} and O_{1s} and may also be expected with PIII treatment. These results confirm the interpretation of the trends observed with Raman and FTIR spectroscopy and also provide some specificity in the description of the chemical changes associated with the PIII treatment.

Further analysis of C_{1s}, O_{1s}, and N_{1s} lines is difficult because of the diversity of structures introduced by the PIII treatment. Figure 6(b,c) shows curve fitting for the C_{1s} high-resolution region spectra with the set of component peaks reported for nylon in the Beamson and Briggs Scienta ESCA300 database.[77] The fitting results of the XPS spectrum for the PIII-treated sample [Fig. 6(c)] are highly uncertain because of the multiplicity of the fitting parameters involved. For this reason, we prefer to view the XPS results as qualitative indicators of structural transformations in nylon during PIII treatment.

The changes from the amide bonding of nylon in the treated surface provide an opportunity to detect amide bonding associated with a surface-immobilized protein. Figures 6–8 show XPS spectra of treated and untreated nylon with and without HRP. The effect of protein attachment can be clearly observed. The C_{1s} shoulder near 288 eV in the spectrum of untreated nylon, attributed to carbon in the amide group of the nylon macromolecule, remains after HRP adsorption because of the contributions of amide groups in the HRP molecule (Fig. 6). However, after the attachment of HRP to a PIII-treated surface, the shoulder at 288 eV reappears because of the presence of amide groups in the attached HRP molecules. The N_{1s} spectrum shows weakly increased intensity in the high-energy shoulder (Fig. 7) after the attachment of HRP to the untreated surface. The attachment of HRP to the PIII-treated surface significantly increases the intensity of the high-energy shoulder associated with the reappearance of amide groups. The attachment of the protein to the untreated surface also slightly increases the high-energy shoulder (Fig. 8) in the O_{1s} region scan. On PIII-treated nylon, the attachment of HRP returns the low-energy shoulder with a strong intensity. Therefore, the spectra of HRP-soaked samples show clearly the presence of attached protein on the untreated and PIII-treated nylon. The fact that evidence for amide bonds appears only in the treated sample exposed to the HRP-containing buffer solution and not in the sample washed in a fresh buffer indicates that the reappearance of amide groups cannot be associated with the removal of the PIII-modified surface layer during the buffer washes.

Another possible strategy for detecting the adsorbed protein layer involves the sulfur peak because this element is present in HRP and is not present in nylon. The HRP molecule has a mass of

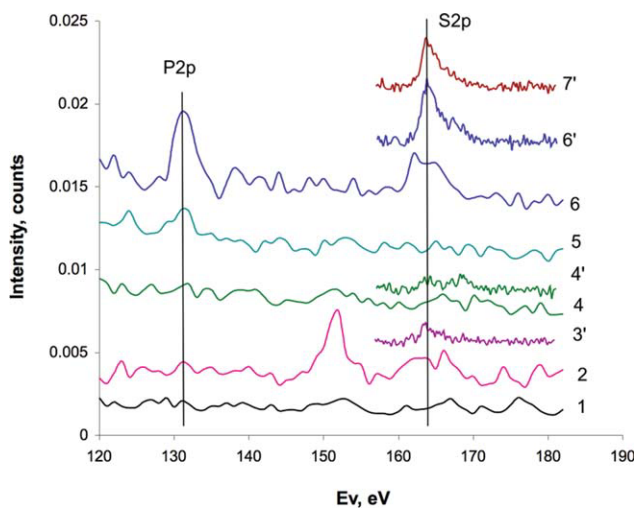

Figure 9 XPS S_{2p} and P_{2p} lines of (1) untreated nylon, (2) untreated nylon incubated in the HRP-containing buffer, (3) untreated nylon incubated in the HRP-containing buffer and washed with Triton X100 detergent, (4) PIII-treated nylon, (5) PIII-treated nylon incubated in the pure buffer, (6) PIII-treated nylon incubated in the HRP-containing buffer, and (7) PIII-treated nylon incubated in the HRP-containing buffer and washed with Triton X100 detergent. The XPS spectra that were recorded with a 30-eV pass energy and 50 scans are marked with apostrophes. The other spectra were recorded with a 160-eV pass energy and 1 scan. [Color figure can be viewed in the online issue, which is available at wileyonlinelibrary.com.]

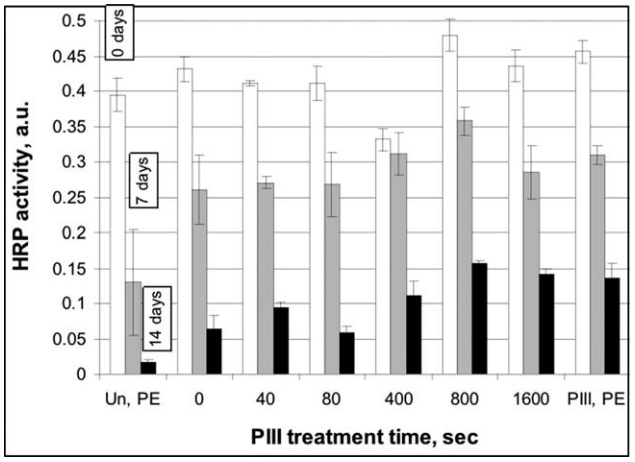

Figure 10 Activity of the attached HRP protein on nylon surfaces modified by the PIII treatment. Results are shown for treatment times of 0, 40, 80, 400, 800, and 1600 s. The controls showed the activity of attached HRP on untreated UHMWPE and PIII-modified UHMWPE (1600-s treatment time).

44 kDa and includes10 cysteine molecules and 7 methionine amino acid molecules, each of which contains 1 sulfur atom. XPS spectra of untreated nylon and PIII-treated nylon do not show sulfur S_{2p} lines above the noise. After incubation in an HRP solution, the surfaces of both untreated and PIII-treated nylon contain sulfur concentrations detectable by XPS (Fig. 9). The S_{2p} lines are clear of the noise level in the spectra. However, quantification is hindered by the low signal-to-noise ratios. The atomic concentration of sulfur calculated from spectra is 0.06% on untreated nylon and 0.10% on PIII-treated nylon. The sulfur peak remains in the XPS spectrum of the PIII-modified nylon after washing in Triton detergent. The same wash removes the sulfur peak from the untreated nylon surface, and this is consistent with removal of the protein. Such a detergent wash disrupts the interactions associated with physisorption but cannot break the chemical bonds. This is consistent with previous results for protein attachment to PIII-treated polyethylene,[7] polystyrene,[8] and polytetrafluoroethylene:[9] there were significant increases in coverage on PIII-treated samples versus untreated controls and covalent bonding between the protein layer and the treated surfaces.

HRP molecules also contain two Ca atoms and one Fe atom in the porphyrin ring. These elements may also be expected in the HRP-attached layer. However, the noise level of the XPS spectra for untreated nylon indicates that the background levels of Ca and Fe are higher than the expected concentrations of these elements. Low levels of Fe and Ca can be detected in the spectra of PIII-treated nylon, most likely because of sputtering from an additional mesh electrode in the PIII system during implantation (Table II). The Fe surface concentration is highest for the PIII-treated sample before exposure to the buffer solution. Fe contamination is decreased after incubation of the modified nylon in the buffer. If the Fe ions are not chemically bound to the modified nylon macromolecules, the P anion from the buffer can accept an Fe cation and remove it from the surface layer into the solution. Therefore, it is likely that much of the deposited Fe is not chemically bound to the modified nylon and may be readily removed. Therefore, the detected Fe does not belong to the HRP molecule.

Na and P species are derived from the buffer (Fig. 9 and Table II). Na is present at an apparently higher concentration than P on the PIII-modified surface. Na may react with carboxylic anions in solution to produce sodium carboxylate via the following pathway:

$$\mathrm{R{-}COOH + Na \rightarrow R{-}COONa} \qquad (9)$$

P anions may react with free radicals:

$$\mathrm{R\cdot + (PO_4)^{-3} + 2Na^{+} \rightarrow R{-}(PO_4)Na_2} \qquad (10)$$

Other reactions with the P anion have a lower probability. The presence of the P anion could alternatively be explained by the diffusion of the ion into the water-swollen volume of the modified surface layer of nylon. The chemical-bonding explanation discussed earlier, however, seems more likely because the rigorous washing process in deionized water should completely remove buffer salt molecules from the swollen layer.

The surface-attached HRP protein shows catalytic activity on the nylon surface, and this is consistent with observations for polyethylene, polystyrene, and polytetrafluoroethylene surfaces (Fig. 10). The protein activity immediately after attachment is similar or slightly lower for the untreated nylon in comparison with the PIII-modified nylon samples. Results that were previously obtained for polyethylene are shown here as controls and for comparison with our current results. The difference in the HRP catalytic activity between the PIII-treated and untreated samples is proportional to the difference in the amount of the attached protein, as determined by XPS.

After 7 and 14 days of storage in the buffer, the activity of the attached protein on all samples decreases. However, the activity of the protein on untreated nylon decreases faster than that on PIII-modified nylon. The highest activity after long-term storage is observed for long-time treatments (high ion fluence). The catalytic activity of protein on nylon surfaces with high fluence behaves similarly to that on modified polyethylene samples treated with the same high ion fluence.[7]

CONCLUSIONS

The complementary combination of FTIR–ATR and XPS has been proved to be effective in the study of both the changes in surface chemistry resulting from the ion implantation of nylon and the detection of a surface-attached layer of the enzyme HRP. The presence of amide bonds in the bulk, unmodified polymer makes the use of the FTIR–ATR method for detecting the surface-bound protein impossible. The near-surface sensitivity of XPS, however, limits the signal to the ion-damaged region in which most of the amide bonding has been eliminated. The reappearance of features in the XPS spectrum associated with amide bonds after HRP attachment, combined with the appearance of a trace sulfur peak, confirms the presence of the attached protein layer. The ability to detect traces of P and Na by XPS also provides additional information about the interaction of the buffer solution with the ion-modified layer.

The results of the combined Raman, XPS, and FTIR–ATR analyses support the view that PIII treatment causes significant structural changes in the surface layer of nylon. Carbonization of the top surface layer and depolymerization in deeper layers occur together with the formation of additional hydroxyl, amine, amino acid, carbonyl, and nitrile groups due to high-energy ion bombardment of nylon. Contact-angle data show that the surface energy and its polar component change significantly in response to PIII treatment. The structural analyses indicate that the changes in surface energy are due to the formation of free radicals and new polar groups on the surface. Structural changes in the surface layer continue to occur for a long time (a month) after the PIII treatment, perhaps because of the diffusion of free radicals and their kinetics.

The nylon surface becomes more favorable for the attachment of protein after PIII. The amount of attached protein and its activity are higher on the modified surface versus the untreated control. The attached protein appears to be stabilized by the PIII-modified layer in terms of long-term catalytic activity. The results of PIII modification and protein covalent attachment for nylon are similar to those observed for polyethylene, polystyrene, and polytetrafluoroethylene systems.[7–9]

References

1. Nylon Plastics Handbook; Kohan, M. I., Ed.; Hanser Gardner: Munich, 1995.
2. Nelson, W. E. Nylon Plastics Technology; Newnes-Butterworths: Markham, Canada, 1976.
3. Bashford, D. Thermoplastics: Directory and Databook; Springer: Berlin, 1997.
4. Biron, M. Thermoplastics and Thermoplastic Composites; Elsevier: Amsterdam, 2007.
5. Handbook of Thermoplastics; Olabisi, O., Ed.; Marcel Dekker: New York, 1997.
6. Pimentel, G. C.; McClellan, A. L. The Hydrogen Bond; Freeman: San Francisco, 1960.
7. Nosworthy, N. J.; Ho, J. P. Y.; Kondyurin, A.; McKenzie, D. R.; Bilek, M. M. M. Acta Biomater 2007, 3, 695.
8. Kondyurin, A.; Nosworthy, N. J.; Bilek, M. M. M. Acta Biomater 2008, 4, 1218.
9. Gan, B. K.; Kondyurin, A.; Bilek, M. M. M. Langmuir 2007, 23, 2741.
10. Odzhaev, V. B.; Kozlov, I. P.; Popok, V. N.; Sviridov, D. B. Ion Implantation of Polymers; Belorussian State University: Minsk, 1998.
11. Fink, D. Fundamentals of Ion-Irradiated Polymers; Springer: Berlin, 2004.
12. Kondyurin, A.; Bilek, M. Ion Beam Treatment of Polymers; Elsevier: Oxford, 2008.
13. Svorcik, V.; Rybka, V.; Vacik, J.; Hnatowicz, V.; Ochsner, R.; Ryssel, H. Nucl Instrum Methods Phys Res Sect B 1999, 149, 331.
14. Toth, A.; Bell, T.; Bertoti, I.; Mohai, M.; Zelei, B. Nucl Instrum Methods Phys Res Sect B 1999, 148, 1131.
15. Popok, V. N.; Azarko, I. I.; Odzhaev, V. B.; Toth, A.; Khaibullin, R. I. Nucl Instrum Methods Phys Res Sect B 2001, 178, 305.
16. Lacoste, A.; Pelletier, J. Nucl Instrum Methods Phys Res Sect B 2003, 208, 260.
17. Veres, M.; Fule, M.; Toth, S.; Pocsik, I.; Koos, M.; Toth, A.; Mohai, M.; Bertoti, I. Thin Solid Films 2005, 482, 211.
18. Mesyats, G. A.; Klyachkin, Y. S.; Garilov, N. V.; Mizgulin, V. N.; Yakushev, R. M.; Kondyurin, A. V. Vacuum 1996, 47, 1085.
19. Gavrilov, N.; Yakusheva, D.; Kondyurin, A. J Appl Polym Sci 1998, 69, 1071.
20. Kondyurin, A.; Karmanov, V.; Guenzel, R. Vacuum 2002, 64, 105.
21. Kondyurin, A.; Naseri, P.; Fisher, K.; McKenzie, D. R.; Bilek, M. M. M. Polym Degrad Stab 2009, 94, 638.
22. Licciadello, A.; Puglisi, O.; Calcagno, L.; Foti, G. Nucl Instrum Methods Phys Res Sect B 1990, 46, 338.
23. Klaumunzer, S.; Zhu, Q. Q.; Schnabel, W.; Schumacher, G. Nucl Instrum Methods Phys Res Sect B 1996, 116, 154.
24. Georhegan, M.; Abel, F. Nucl Instrum Methods Phys Res Sect B 1998, 143, 371.
25. Evelyn, A. L.; Ila, D.; Zimmerman, R. L.; Bhat, K.; Poker, D. B.; Hensley, D. K.; Klatt, C.; Kalbitzer, S.; Just, N.; Drevet, C. Nucl Instrum Methods Phys Res Sect B 1999, 148, 1141.
26. Netcheva, S.; Bertrand, P. Nucl Instrum Methods Phys Res Sect B 1999, 151, 129.
27. Zaporojtchenko, V.; Zekonyte, J.; Wille, S.; Schuermann, U.; Faupel, F. Nucl Instrum Methods Phys Res Sect B 2005, 236, 95.
28. Kondyurin, A.; Gan, B. K.; Bilek, M. M. M.; Mizuno, K.; McKenzie, D. R. Nucl Instrum Methods Phys Res Sect B 2006, 251, 413.
29. Zhang, J.; Yu, X.; Li, H.; Liu, X. Appl Surf Sci 2002, 185, 255.
30. Parada, M. A.; Delalez, N.; de Almeida, A.; Muntele, C.; Muntele, I.; Ila, D. Nucl Instrum Methods Phys Res Sect B 2006, 242, 550.
31. Schiller, T. L.; Sheeja, D.; McKenzie, D. R.; McCulloch, D. G.; Lau, D. S. P.; Burn, S.; Tay, B. K. Surf Coat Technol 2004, 177, 483.
32. Colwell, J. M.; Wentrup-Byrne, E.; Bell, J. M.; Wielunski, L. S. Surf Coat Technol 2003, 168, 216.
33. Suzuki, Y.; Iwaki, M.; Tani, S.; Oohashi, G.; Kamio, M. Nucl Instrum Methods Phys Res Sect B 2003, 206, 538.
34. Mesyats, G.; Klyachkin, Y.; Gavrilov, N.; Kondyurin, A. Vacuum 1999, 52, 285.
35. Satriano, C.; Scifo, C.; Marletta, G. Nucl Instrum Methods Phys Res Sect B 2000, 166, 782.

36. Ueda, M.; Kostov, K. G.; Beloto, A. F.; Leite, N. F.; Grigorov, K. G. Surf Coat Technol 2004, 186, 295.
37. Ektessabi, A. M.; Yamaguchi, K. Thin Solid Films 2000, 377, 793.
38. Mizuno, K.; Gan, B. K.; Kondyurin, A.; Bilek, M. M. M.; McKenzie, D. R. Plasma Processes Polym 2008, 5, 834.
39. Hong, W.; Woo, H.-J.; Choi, H.-W.; Kim, Y.-S.; Kim, G. Appl Surf Sci 2001, 169, 428.
40. Biersack, J. P.; Kallweit, R. Nucl Instrum Methods Phys Res Sect B 1990, 46, 309.
41. Pignataro, B.; Fragala, M. E.; Puglisi, O. Nucl Instrum Methods Phys Res Sect B 1997, 131, 141.
42. Compagnini, G.; Angilella, G. G. N.; Raudino, A.; Puglisi, O. Nucl Instrum Methods Phys Res Sect B 2001, 175, 559.
43. Kondyurin, A. V.; Maitz, M. F.; Romanova, V. A.; Begishev, V. P.; Kondyurina, I. V.; Guenzel, R. J Biomater Sci Polym Ed 2004, 15, 145.
44. Kondyurin, A.; Romanova, V.; Begishev, V.; Kondyurina, I.; Guenzel, R.; Maitz, M. F. J Bioact Compatible Polym 2005, 20, 77.
45. Dejun, L.; Jie, Z.; Hanqing, G.; Mozhu, L.; Fuqing, D.; Qiqing, Z. Nucl Instrum Methods Phys Res Sect B 1993, 82, 57.
46. Wong, K. H.; Zinke-Allmang, M.; Wan, W. K.; Zhang, J. Z.; Hu, P. Nucl Instrum Methods Phys Res Sect B 2006, 243, 63.
47. Murphy, J. J.; Patel, M.; Powell, S. J.; Smith, P. F. Radiat Phys Chem 2002, 63, 101.
48. San, J.; Wang, Z.; Li, S.; Liu, J. Surf Coat Technol 2006, 200, 5245.
49. Fu, R. K. Y.; Cheung, I. T. L.; Mei, Y. F.; Shek, C. H.; Siu, G. G.; Chu, P. K.; Yang, W. M.; Leng, Y. X.; Huang, Y. X.; Tian, X. B.; Yang, S. Q. Nucl Instrum Methods Phys Res Sect B 2005, 237, 417.
50. Kumar, R.; Prasad, R.; Vijay, Y. K.; Acharya, N. K.; Verma, K. C.; De, U. Nucl Instrum Methods Phys Res Sect B 2003, 212, 221.
51. Balasubramanian, V.; Kelkar, D. S.; Kurup, M. B. Nucl Instrum Methods Phys Res Sect B 1996, 113, 257.
52. Popok, V. N.; Odzhaev, V. B.; Azarko, I. I.; Kozlov, I. P.; Sviridov, D. V.; Hnatowicz, V.; Vacík, J.; Cervená, J. Nucl Instrum Methods Phys Res Sect B 2000, 166, 660.
53. Popok, V. N.; Odzhaev, V. B.; Kozlov, I. P.; Azarko, I. I.; Karpovich, I. A.; Sviridov, D. V. Nucl Instrum Methods Phys Res Sect B 1997, 129, 60.
54. Popok, V. N.; Azarko, I. I.; Odzhaev, V. B.; Tóth, A.; Khaibullin, R. I. Nucl Instrum Methods Phys Res Sect B 2001, 178, 305.
55. Kondyurin, A.; Volodin, P.; Weber, J. Nucl Instrum Methods Phys Res Sect B 2006, 251, 407.
56. MacDonald, C.; Morrow, R.; Weiss, A. S.; Bilek, M. M. M. J R Soc Interface 2008, 5, 663.
57. Do, C. H.; Pearce, E. M.; Bulkin, B. J.; Reimschuessel, H. K. J Polym Sci Part A: Polym Chem 1987, 25, 2301.
58. Thanki, P. N.; Singh, R. P. Polymer 1998, 39, 6363.
59. Steinhauser, H.; Ellinghorst, G. Angew Makromol Chem 1984, 120, 177.
60. Yasuda, H. Luminous Chemical Vapor Deposition and Interface Engineering; Marcel Dekker: New York, 2005.
61. Weikart, C. M.; Yasuda, H. K. J Polym Sci Part A: Polym Chem 2000, 38, 3028.
62. Canal, C.; Molina, R.; Bertran, E.; Erra, P. J Adhes Sci Technol 2004, 18, 1077.
63. Rangel, E. C.; Gadioli, G. Z.; Cruz, N. C. Plasmas Polym 2004, 9, 35.
64. Yasuda, H.; Sharma, A. K.; Yasuda, T. J Polym Sci Polym Phys Ed 1981, 19, 1285.
65. Gagnon, D. R.; McCarthy, T. J. J Appl Polym Sci 1984, 29, 4335.
66. Steinhauser, H.; Ellinghorst, G. Angew Makromol Chem 1984, 120, 177.
67. Povstugar, V. I.; Kodolov, V. I.; Mikhailova, S. S. Composition and Properties of Surfaces of Polymer Materials; Khimiya: Moscow, 1988.
68. Encyclopedia of Polymer Science and Technology; Herman, M. F., Ed.; Wiley: New York, 2004.
69. Ostrovskaya, L.; Perevertailo, V.; Ralchenko, V.; Dementjev, A.; Loginova, O. Diamond Relat Mater 2002, 11, 845.
70. Kawamura, H.; Osedo, H. J Electrochem Soc 2008, 802, 720.
71. Tessier, P. Y.; Pichon, L.; Villechaise, P.; Linez, P.; Angleraud, B.; Mubumbila, N.; Fouquet, V.; Straboni, A.; Milhet, X.; Hildebrand, H. F. Diamond Relat Mater 2003, 12, 1066.
72. Papirer, E.; Brendle, E.; Ozil, F.; Balard, H. Carbon 1999, 37, 1265.
73. Carbon Nanotubes: Preparation and Properties; Ebbesen, T. W., Ed.; CRC: Boca Raton, FL, 1996.
74. Lang, N. D.; Kohn, W. Phys Rev B 1970, 12, 4555.
75. Metal Matrix Composites; Johnson, W. S., Ed.; ASTM International: West Conshohocken, PA, 1989.
76. Tsukada, M.; Tsuneyuki, S.; Shima, N. Surf Sci 1985, 164, L811.
77. Beamson, G.; Briggs, D. High Resolution XPS of Organic Polymers: The Scienta ESCA300 Database; Wiley: Chichester, England, 1992.